Brachiating Monkey Robot

Samuel Bednarski, Michael Dermksian, Vybhav Murthy,
Nataliya Rokhmanova, Michael Turski
24-775 Robot Design & Experimentation

Abstract:

Brachiation is a swinging locomotive strategy typically performed by primates. Primates' use of their elbows allows them to easily traverse wooded terrain and swing to higher heights, which could be a useful skill for a robot. Current brachiating robots often have a single straight arm link and have only been tested on a flat horizontal ladder. It is not yet known how a brachiating robot can benefit from a powered elbow joint; whether, when compared to a single arm link robot, it is more efficient to swing across flat horizontal bars; or if it will enable the robot to climb to higher heights. We developed and tested a robot with a powered elbow joint to evaluate its ability to traverse across an inclined horizontal ladder. The implementation on the physical prototype verified that the robot can traverse flat, horizontal monkey bars. Experiments on the simulated robot demonstrate that the robot with the powered elbow enabled it to reach higher grounds versus a similar robot with no elbow.

Introduction:

The brachiation of primates is a swinging locomotive strategy that permits the animal to swing through the forest canopy and maneuver from tree to tree without having to descend to the ground (Fig 1). This kind of maneuver is of interest to roboticists interested in swinging robots that can traverse man-made structures with regularly-spaced handholds, such as bridges or buildings, as well as natural environments like tree branches. Robots that are able to brachiate can enable traversing irregular or dangerous ground by traveling above it instead, thus permitting more robust search-and-rescue missions, maintenance, construction, or environment exploration. There are no robots currently capable of traversing this type of terrain.

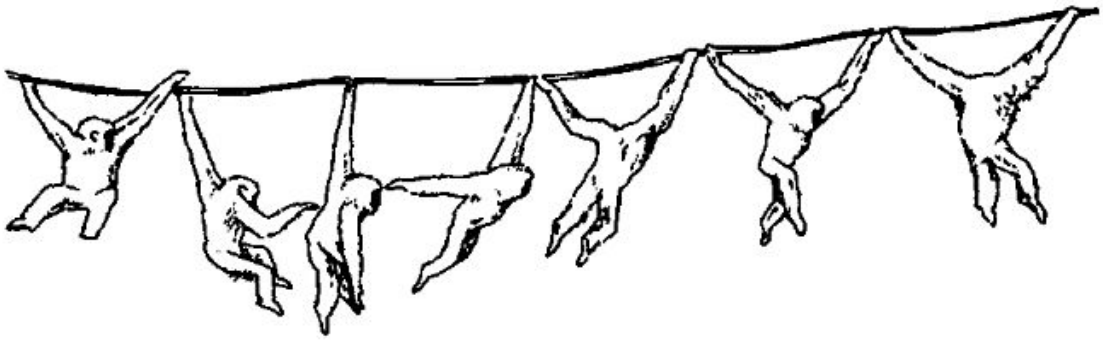

Fig. 1: The brachiation of primates resembles a pendulum, and enables them to swing to higher hand holds. Image taken from [1].

In continuous contact brachiation, where at least one hand is holding at any point in time, the pendular exchange between kinetic and gravitational potential energy is leveraged. A swing is initiated with the back arm in a pull-up position, which serves to elevate the center of gravity, enabling the animal to rise high at the end of the support phase, thus permitting a greater vertical displacement and therefore greater acceleration due to gravity. During swing, the stance arm is adducted and the elbow is flexed, which reduces the arm's moment of inertia and enables a rapid recovery.

Brachiation is a challenging robotics problem, in part due to its underactuated control: the robot can't provide torques at the handhold. The first brachiation robot to make use of energy stored by swing was a five joint, six link robot designed by Fukuda, Hosokai and Kondo in 1991 [2]. Yamafuji and colleagues [3] simplified the initial robot by designing and building a two-link brachiator controlled by a single actuator at the central link, using a proportional-derivative controller to implement a prescribed reference trajectory for the two links. Spong et al. then developed a controller that could allow a similar two-link robot with a single center-position actuator to swing up from a stable equilibrium to an inverted position [4]. These developments were foundational to the later work of Fukuda and Saito, who implemented these principles in the Brachiator II, which was a two-link brachiation robot in the form of a double pendulum with grips at either end [5]. They were able to swing and catch across a horizontal ladder, using an heuristic learning process and swing amplitude control. More complex brachiators include the Gorilla Robot II from Kajima et al., a 19-link robot with 20 actuators that successfully brachiated using two distinct continuous gaits: over-hand and side-hand [6]. Recent efforts to improve brachiation ability have included the addition of a waist [7] as well as control to traverse a flexible cable [8]. Most recently, Yang et al. designed a three-link brachiation robot that uses an optimal control based trajectory tracking controller, and were able to simulate and test successful brachiation across monkey bars [9]. Our prototype directly extends the research presented by Yang et al., and features nearly all the same hardware with the addition of a powered elbow.

However, none of the five-link brachiator robots described here implement an active elbow joint that enables the robot to swing up to a higher bar with each cycle. In brachiators, the flexion of the elbow serves to elevate the center of gravity to enable the animal to rise higher at the end of the support phase for the purpose of permitting a greater drop and therefore greater acceleration due to gravity during the following cycle. Incorporating this kind of behavior in a robot would permit the robot to traverse more complex or variable terrains.

In order to address this gap in current knowledge, we aimed to build a brachiating robot that includes a powered elbow joint. We first simulated and designed the control strategy for the robot, then fabricated and assembled it. We tested the robot on a physical test rig and in simulation to evaluate the effect of an actuated elbow on its ability to successfully brachiate across bars at varying inclines.

Research Question:

How can the addition of an elbow joint affect a brachiating robot's ability to swing to a higher ground? We aimed to answer this question both physically and in simulation. In real-life testing, we hypothesized that at a given angle of incline, there are optimal rung spacings and swing trajectories that allow the robot to successfully complete a successful brachiation cycle. In simulation, we hypothesize that at these previously determined angles of incline and bar spacings, a robot with a powered elbow will complete more successful consecutive brachiation cycles than the same robot with a locked-out elbow motor.

Final Design:

The final design presented herein is largely an extension of the work done by Yang et. al. [9]. The CAD model for the robot is depicted next to the final prototype in Fig 2. The design features a rectangular torso link that houses the logic board and battery. Two shoulder motors are affixed to the top of the robot and are connected to two elbow motors via a rigid link. The two elbow motors are further connected to the actuated gripper mechanisms by a second set of rigid links. The grippers each use a single servo motor to open and close the fingers of the

linkage. Hollow shaft motors and hollow tubing are utilized to route wiring through the center of each axis of rotation so that the swinging links would not become entangled during trajectory execution.

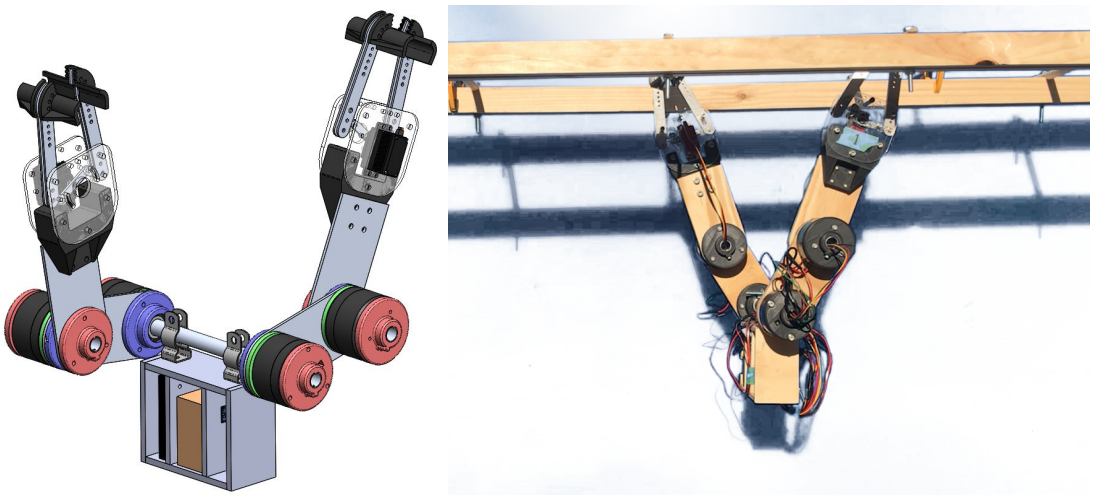

Fig. 2 The final CAD design (left) and the final robot design (right).

The four motors actuating the shoulders and elbows are the DJI RoboMaster GM6020. The impetus for selecting these motors comes largely from the direct recommendation of Yang et. al., who utilized the same motors in their elbowless design [9]. Additionally, the motors interface conveniently with the RoboMaster Development Board Type A, which features an STM32 programmable microcontroller. The gripper motors, along with the associated linkages, were lifted directly from the aforementioned elbowless design.

The trajectory optimization process, described further below, showed that a wide range of link lengths are feasible for achieving successful brachiation with our motors. We performed a combinatorial approach to selecting optimal link lengths by analyzing combinations of 4 potential forearm and 4 upper arm lengths with two heuristics: 1. Analyzing swing patterns for feasibility and gripper placement, 2. Analyzing trajectory data. We began by decreasing the maximum possible torque the motors could apply, until half of the combinations were unable to find solutions. Trajectories generated for the remaining combinations were then analyzed so that the robot did not hit the bars, and the final lengths were selected for their minimal average and peak torques used. The final link lengths are 105mm for the upper arm and 267mm for the lower arm.

The simple control architecture utilizes two PID controllers to track the trajectory generated offline via the trajectory optimization. To further reduce the complexity of the design, only the angular positions and velocities of the joints are tracked, while the angle, horizontal position and vertical position of the body are not considered. The controller also takes advantage of a feedforward torque term taken from the optimized trajectory. These controllers were tested in simulation using Simulink, and showed acceptable tracking performance with only modest deviations in the uncontrolled states of the robot. A third PID controller is necessary on the physical controller to translate torques generated by the aforementioned feedback and feedforward terms into voltages for the motors. The advantage of such an architecture is its ease of implementation on a low-level processor such as the STM32 and the speed of the associated calculations (in comparison to a higher-order feedback controller).

In the initial project document, we proposed two stretch goals: to achieve several continuous brachiation cycles and to implement momentum generation such that the monkey could start with both hands on a single bar. We did not achieve any stretch goals on the

physical robot, but we were able to achieve a continuous brachiating gait in simulation via trajectory optimization. We believe that the hardware and software are in a state that would allow these trajectories to be executed, but were unable to complete them as the original test plan was of higher priority.

Trajectory Optimization:

In order to generate swing trajectories for the robot, we used a hybrid trajectory optimization, which first involved setting up a hybrid system for our model to include the notion of contact with the environment. This was done by solving for the robot's dynamics, position and velocity constraints, reset maps, and guard conditions for each contact mode: left arm, right arm, and both arms. With this hybrid system model for our robot, we were able to set up a hybrid trajectory optimization framework to generate swing trajectories that take into account the robot's contact with the monkey bars.

For our physical testing and simulation testing, we generated trajectories to minimize the torque used by the robot, and added constraints to force the robot to stay underneath the monkey bars. If left unconstrained, some trajectories will allow the robot to move its forearm through the monkey bars during the swing. Constraints were also added to enforce the motor model, and to specify an underhand swing motion if desired. Finally, the swing trajectory was solved for using three stages: (1) Initialize with first order fit and solve with a constant cost function. (2) Transition the problem to a third order fit for the states, a zero order hold for inputs and apply the cost function for minimizing torque input. (3) Repeat (2), but seed this optimization with an adjustable, small deviation from the result of (2), in order to avoid finding a local minima.

This trajectory optimization framework was written such that the size of timesteps are a decision variable in the optimization; therefore, the size of the timesteps vary, so we must post-process the trajectory in order to easily run the trajectory on the robot. The trajectory is interpolated using a third order fit on the robot's states, and a zero-order hold on the control inputs. Both the states and controls are interpolated using a 1ms timestep in order to directly run the trajectory on the robot.

Methods:

In order to evaluate our research question, we established an experimental protocol to evaluate our hypotheses both on a physical test rig and in simulation (Fig 3). Testing the physical robot allows us to evaluate whether our build and control strategy are appropriate for a brachiating robot. In simulation, we are able to make a more controlled comparison between a robot with a powered elbow and one with the elbow locked out, holding all other variables constant.

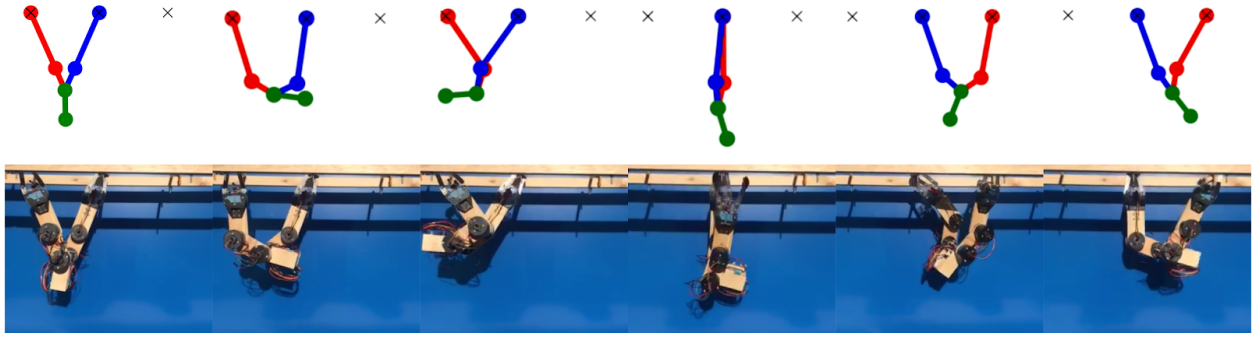

Fig 3. A sagittal view of our simulated robot (top) and physical build (bottom) successfully completing the same single brachiation cycle.

Physical Testing

To test the robot on a physical rig, we built a wooden test platform (Fig 4). The monkey bar test rig is 8ft in length, 4ft in height, and 1ft in width. These dimensions were selected to accommodate the maximal range of our robot's size. The rungs are 0.5in in diameter to match the grippers, and their spacing can be freely adjusted as they move along the sliders and are locked in place. In order to incline the bars, one side of the rig was raised on sturdy boxes until it reached the desired angle. Angle of incline was confirmed with two digital IMU levels.

The physical testing plan was to generate appropriate trajectories for level swinging and execute them with the designed hardware and software. Successful execution would primarily demonstrate the quality of the design. It would secondarily serve to validate the quality of the simulation - indicating that simulated results are also practicable on a physical platform. Further testing could then be executed in simulation with the assumption that simulated results could feasibly be executed in hardware. If the monkey was capable of level swinging, inclined swings would be attempted.

The physical platform was qualitatively evaluated through pass/fail data and relevant observations. The general strategy for trajectory execution was as follows. The robot was placed on the level (0 degree) test rig and allowed to passively hang. The controller was then engaged to bring the monkey into an appropriate initial condition and the trajectory was subsequently executed. A swing was considered successful if the robot was able to release its gripper from the back rung and close it around the forward rung without falling. Three successful swings was considered sufficient to demonstrate the robot's overall success for the level test rig.

Fig. 4: The experimental rig is made of wood and has adjustable rung spacing.

Simulation Testing

To test the robot in simulation, we made use of our full physics model and the actual robot dimensions and inertias. At the 0.3m bar spacing which we evaluated on our physical test rig, and varying angles of incline, we simulated two conditions: one where the robot is actuated as normal, and one where the elbow motor is locked out such that there is just one continuous arm piece rather than a forearm and upper arm. We evaluated angles of elevation from 0 to 30 degrees of incline. A brachiation trajectory was optimized for each of these conditions. We then compared success and torques required between both conditions; success is defined by whether a stable trajectory was found.

Physical Testing Results

Only the 0 degree incline was successfully tested using the physical prototype. In order to successfully catch the bar at no incline, trajectories based on a 10 degree incline were used.

This slight incline can be seen in Figure 3. An inclined trajectory was necessary because the robot often undershot the target bar due to sideways rotation, causing it to miss and fail. The robot successfully executed this trajectory three times. With this success, we attempted inclined testing with the test rig at 5 degrees, but were unable to achieve successful inclined swings before the robot damaged itself, abruptly ending testing. We are not able to conclusively evaluate our physical testing hypothesis.

With further testing, we believe we would be able to successfully execute inclined swings with the current robot platform. We also believe it would be possible to use sensor data on the physical robot to evaluate whether the angle of incline has a significant increase on elbow torques. This is a logical extension of our present research question, that an elbow motor enables a robot to swing up an incline. If the elbow is indeed assisting incline brachiation, we may expect to see a greater magnitude of elbow motor torques as the incline increases. However, we presently do not have enough sample points on incline data in physical testing to perform a well-powered statistical analysis.

Simulation Testing Results

For the monkey with powered elbows (five-link model), feasible swinging motions were found via trajectory optimization for bar elevation angles from 0 degrees up to 30 degrees using the overhand motion. For all angles simulated, at least one trajectory was found which meets the torque constraints of our physical prototype. In contrast, feasible trajectories for a similar monkey model with no elbows (three-link model) were only found for inclines from 0 degrees up to 2 degrees, also using an overhand motion. For the no-elbow model, a feasible underhand trajectory could only be found for 0 degree incline.

For the model with powered elbows, overhand trajectories were found to require less torque than underhand trajectories. The opposite is true for the model with no elbows, in which underhand trajectories are more efficient. For the incline angles in which both versions produced a feasible overhand trajectory, the monkey with powered elbows is able to find feasible trajectories with less torque than the monkey with no elbows (Fig. 5). Based on these results, there is some evidence to confirm our hypothesis that powered elbows enable brachiating robots to swing higher, as the powered elbow model was able to find trajectories at inclines that the no-elbow model could not reach.

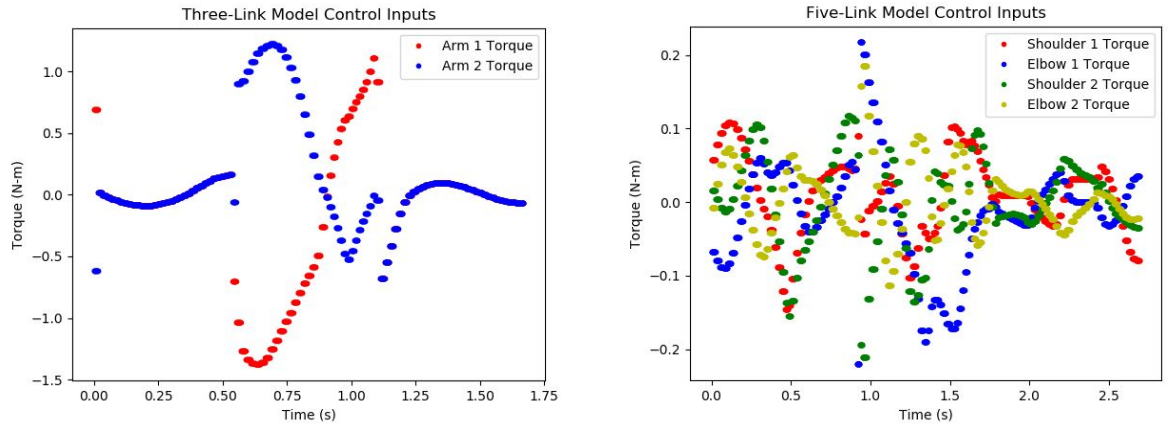

Fig. 5: A sample comparison between the torques needed to execute a single brachiation cycle using an overhand strategy at a 2 degree incline. The powered elbow (right) enables the robot to swing using much less torque than when there is no elbow (left).

Some attempts were made to achieve continuous brachiation in simulation as well. We were able to find feasible trajectories for the powered elbow model up to a 10 degree incline. In one particular case the maximum torque was found to be 0.65 Nm, well within the physical robot limitations (Fig. 6). However, feasible trajectories for continuous brachiation are not solved as easily as single swings, so this was the highest angle achieved in simulation.

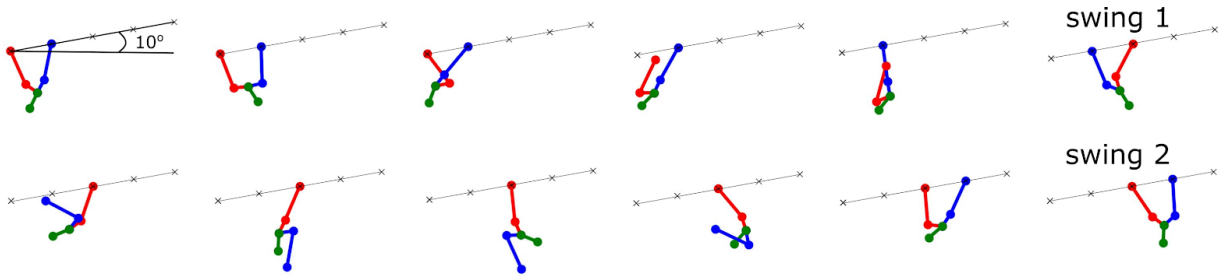

Fig. 6: The five-link model was able to continuously brachiate up a 10 degree incline using an underhand strategy. The top row shows the first swing, until contact is first made, and the second row shows the second swing.

Our methods of evaluating our hypotheses are subject to limitations. Testing in simulation does not necessarily translate to real-world conclusions, as the simulation environment makes several simplifying assumptions about the physics of the world as well as our robot's dimensions and weight. We would expect that in implementation, more intervening variables would result in a lower rate of success than that shown in our results. Additionally, simulating an identical robot with the elbow locked out is not necessarily a "fair" comparison of whether the addition of an elbow enables more successful brachiation. In implementation, a robot designer would likely make use of the cost saved by not including an elbow motor by using more powerful shoulder motors, a condition which is not modeled in our experiment.

Benchmarking Against Biological Inspiration

As this project was inspired by the ability of gibbon monkeys to brachiate with incredible skill and power, we were interested in seeing how our robot powered by the GM6020 motors compares to a gibbon's physiological elbow and shoulder. The vertebrate musculoskeletal system is actuated by a number of muscle-tendon complexes spanning joints that generate forces to flex, extend, or rotate the limb as they contract. In other words, we aimed to evaluate how the calculated joint torques that follow a predefined trajectory compare to the torques that a (very simplified; planar) gibbon would need to exert in order to follow that same trajectory.

To compare how physiological torques compare to mechanical torques, we created a simplified model of the gibbon in the sagittal plane, actuated by the main flexor and extensor muscles of the shoulder and elbow. The six muscles listed in Table 1 (Appendix) comprise approximately 80% of the flexion and extension mass of the Siamang gibbon [10]. Physiological cross-sectional area (PCSA) was determined from cadaveric studies by Michilsens et al. and reproduced here for reference.

PCSA is directly related to the force-generating capacity of all muscles. Maximum contractile force (F_{max}) is found by multiplying PCSA (in m^2) by the maximal isometric stress of a vertebrate muscle, found to be 0.3MPa [12]. F_{max} is then multiplied by the moment arm of the muscle to compute the torques these muscles would generate about the elbow and shoulder while executing our optimal horizontal swinging trajectory at 0.3m bar spacing. To compute how

the muscle moment arms change with angle, we referenced the work of Thorpe et al. [11] in quantifying cadaveric chimpanzee moment arm lengths over a range of motion. Thorpe provides regression equations for calculating moment arms for the major flexor and extensor muscles. Moment arms were calculated at every time step for the physically tested trajectory, in radians. Computed moment arms were then scaled linearly to compensate for the size difference between common chimpanzee and Siamang gibbon forelimb mass. Torques across the trajectory were computed from the F_{max} and scaled moment arms, where flexion is designated as positive torque. Maximum isometric contraction torque was quantified at the peak moment arm angle, which can be thought of as the physiological equivalent of a motor's stall torque.

Maximum isometric contraction torques were 21.6Nm and 27.5Nm for the shoulder flexor and extensors respectively, and 12.1Nm and 6.0Nm for the elbow flexors and extensors respectively. The estimated elbow and shoulder torques across the optimal robot trajectory are shown in Figs. 7 and 8 below. The estimated physiological trajectory torques are approximately one order of magnitude greater than the torques used as control input to our robot. Furthermore, these internal torques, in particular the shoulder torques, are substantially greater than external torques found by Chang et al. as a white-handed gibbon brachiated across instrumented handholds [13]. Though internal torques are not computed *in vivo*, as this requires invasive sensing, the discrepancy between computed external torque experimental values may suggest that the trajectory generated by our robot would be quite strenuous for a typical brachiator.

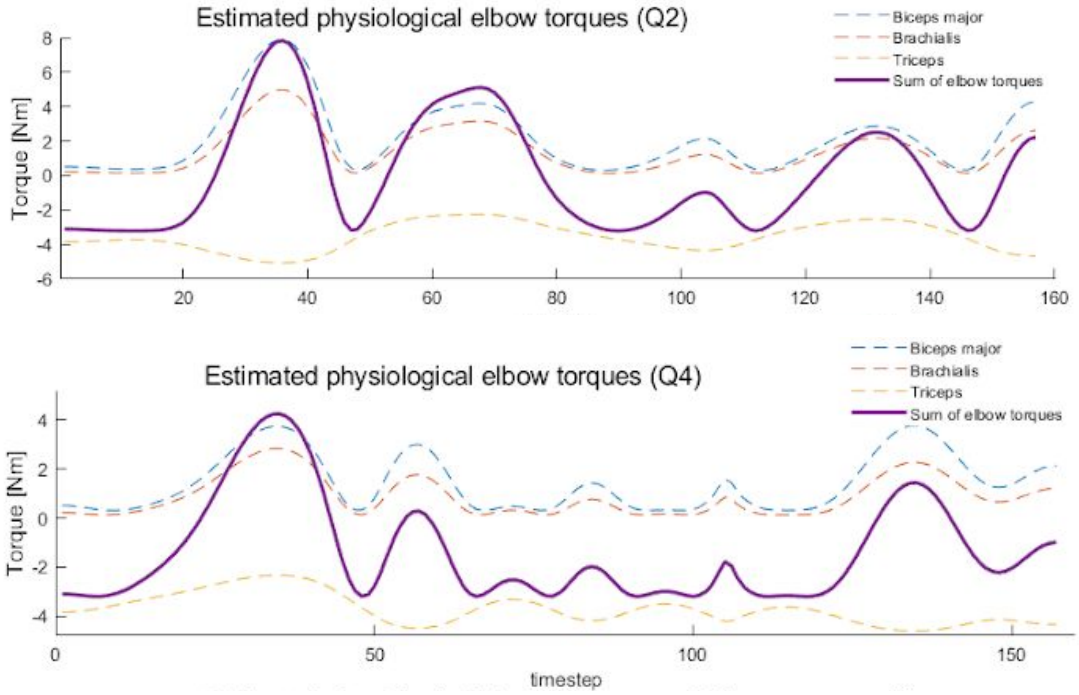

Fig. 7 Estimated gibbon elbow torques to follow the generated trajectory successfully implemented on our physical robot. Here Q2 corresponds to the swinging arm and Q4 is the supporting arm.

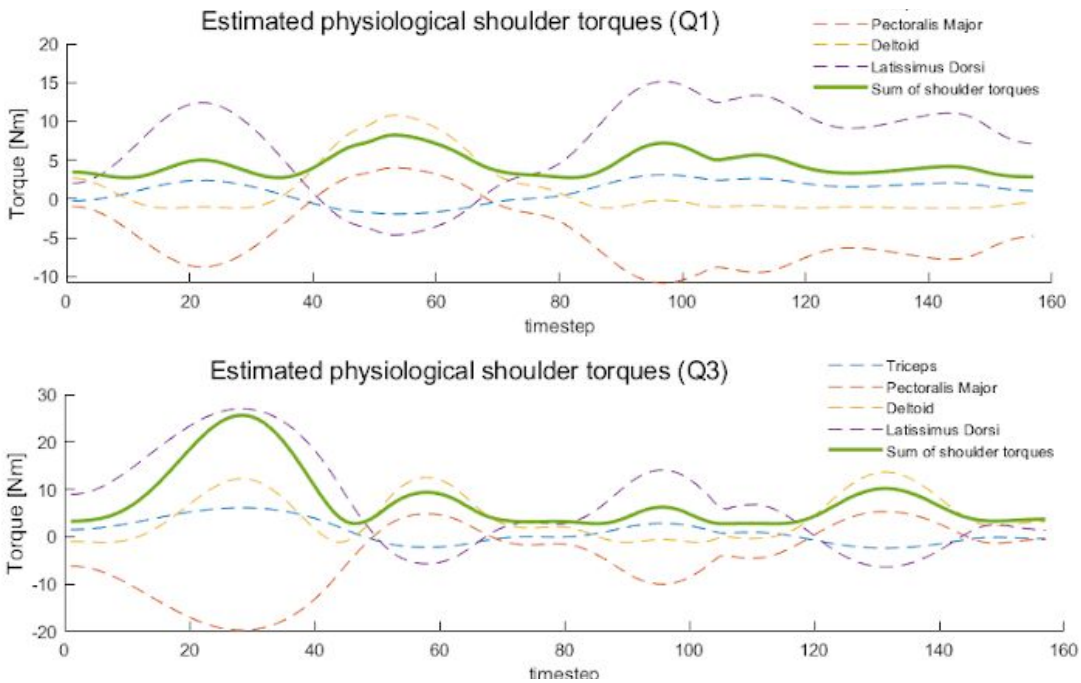

Fig. 8 Estimated gibbon shoulder torques to follow the generated trajectory successfully implemented on our physical robot. Here Q1 corresponds to the swinging arm and Q3 is the supporting arm.

However, these estimates can be refined further by addressing several key limitations. The simplified model uses a limited number of muscles that do not account for all flexion and extension movement, and rotation is not considered. Addition of redundant muscles and another degree of freedom would likely result in a greater estimated torque using the method described here. This method used is albeit an inexact representation of vertebrate musculoskeletal control. Here we assume that the animal uses maximal contraction (F_{max}) throughout the swinging cycle, and is maximally co-contracted throughout (all flexors and extensors active simultaneously), which likely not a plausible control strategy. In reality, muscle contraction is subject to tonic neural activation and its contractility is dependent on a force-length-velocity relationship, neither of which are modeled here. In addition, the redundancy and high-dimensionality of the muscular control space makes solving for muscle activation an indeterminate problem. An extension of this work would be to make use of musculoskeletal forward dynamic modeling approaches in order to generate a best guess as to how a gibbon would recruit its muscles while following our specified trajectory.

Individual Technical Contributions:

Samuel Bednarski: Designed the overall embedded system firmware in C which largely encompassed discrete-time PID implementation and trajectory file parsing. The firmware includes a Bluetooth interface enabling the robot to be modified and controlled quickly which allows tuning and testing to be performed with minimal interruptions between experiments.

Michael Dermksian: Analyzed the unconstrained rigid body dynamics of the system to generate a dynamic model of the robot for trajectory optimization, simulation, and controller design. Dynamic modeling was performed using forward kinematics and Lagrangian mechanics. Calculations were done using MATLAB's symbolic toolbox and were subsequently converted into functions for use in simulation and controller design in Simulink.

Vybhav Murthy: Analyzed different control system techniques; including traditional PID, cascade PID, and double (position and velocity) PID with feedforward that were then implemented on the dynamic model in Simulink for validation. The double PID controller with feedforward proved to track the optimal trajectory more precisely and accurately, and was chosen to be implemented onto the robot.

Nataliya Rokhmanova: Generated a simplified musculoskeletal gibbon model and computed trajectory torques using anatomical values from cadaveric data. Found that the physiological estimates of torque are greater than expected or found in literature, suggesting that the optimal trajectory found by the robot does not correlate to optimal biological swinging behavior. Also built the adjustable test rig, which enabled physical testing.

Michael Turski: Extended the unconstrained dynamical model into a hybrid systems framework. Used trajectory optimization to perform a grid search across the forearm and humerus link lengths to determine the final configuration for the robot and to generate swing behaviors for the physical robot. Finally, using trajectory optimization, performed a comparison of the five-link and three-link robots for different angles of inclined monkey bars.

Conclusions and Next Steps:

The final robot prototype is minimally sufficient to experiment with and test our hypothesis. It was capable of executing successful level swings, but cannot yet perform inclined swings. It also was only able to perform level swinging when supplied an inclined trajectory. This indicates that significant design changes would be necessary to confirm or reject our hypothesis in hardware rather than simulation.

Though our hypothesis could not be fully validated with the physical prototype, some conclusions can be drawn from the simulations. We found that a brachiating robot with powered elbows is able to feasibly swing higher than a similar robot with no elbows. The addition of elbows also seemed to reduce the overall torque requirement as well. Therefore our research question is partially answered, as a powered elbow appears to aid a robot's ability to swing to a higher bar, if only in simulation.

Some improvements could be made to make the design more robust, such as replacing the fragile wooden components with aluminum. Additionally, a better gripper could have been designed which could have relieved some of the limitations of the current prototype. The grippers do not open very wide, so some of the trajectories generated cannot be achieved with the physical model.

Another severe limitation is the quality of the physical model relative to the software model. The wooden links were made by hand and measured with imprecise gauges. As a result, the masses, lengths, and moments of rotational inertia are not exactly matched. The damping coefficients at the joints in simulation are also estimations of the actual parameters. These imprecisions all combine to reduce how results from simulation can be extended to reality. This

mismatch is amplified by the fact that the simulated model is assumed to be planar. While the physical model was designed to move primarily in the sagittal plane, it still exhibits significant out-of-plane translation and rotation.

A final limitation lies in the choice and implementation of our controller. A simple PID controller is used to control the position and velocity of the four arm joint angles. However, three states of the robot are uncontrolled via the current scheme: the angle, vertical position, and horizontal position of the torso. As a result, the current controller is incapable of tracking all states of the optimal trajectory. Additionally, no filtering is applied to the sensor signals. A more sophisticated, higher-order controller and observer such as a linear quadratic Gaussian would likely improve the tracking capabilities (assuming the plant model is accurate).

Though some concrete results were found through simulation, it would have been preferable to validate these results with the physical model as well. First, a statistical approach to evaluating successful brachiation should be employed. We have shown that the robot is capable of brachiating at a 0° incline consistently, but did not run enough trials to generate a statistical success rate. The same type of analysis would be employed for brachiation at upward angles. Additionally, comparisons could be made to a similar brachiation robot with no powered elbows to finally test our hypothesis against. This would be sufficient for us to make any kind of conclusion towards our hypothesis. Beyond this, we would also have liked to achieve continuous brachiation, as opposed to only being able to swing once at a time.

An important realization for our team came from the comparison between a realistic gibbon and our robot model. Rather than developing trajectories that were physiologically inspired, the trajectories optimized for our robot were constrained by the motor parameters, which were in turn constrained by cost and access. As a result, we found that our trajectories and torque limitations do not compare well to our estimates of how a gibbon would perform in similar situations. Brachiators initiate swing with the back arm in a pull-up position, which serves to elevate the center of gravity and increase potential energy. Our optimal trajectory showed slight flexion of the back arm but mainly relied on the swinging of the body at the shoulders in order to generate the momentum necessary to swing successfully. Even though our robotic design is inspired by the gibbon, there is certainly more we can learn from taking a closer look at their behaviors.

Budget:

Below is a preliminary budget for this project. The costs of components marked as “Reusable” reflect a 50% discount. Some components that have been borrowed are included but do not contribute to the budget cost.

Component	Quantity	Total Cost	Note
TOTAL		**$590**	
Aluminum robot arms	4	$220	
Shoulder motors	2	$180	Reusable
Shaft bearings	4	$38	
Battery	2	$35	Reusable
Robot hardware	-	$30	
Test rig hardware	-	$28	
Test rig wood	-	$23	
Motor shaft material	1	$21	
Wooden robot body	1	$5	
Wooden robot arms	4	$5	
Bluetooth transceivers	2	$5	
Elbow actuators	2	$0	Borrowed
Gripper servo assemblies	2	$0	Borrowed
Controller	1	$0	Borrowed
Wires	-	$0	
3D printed motor couplings	16	$0	

References:

[1] E. L. Simons, “Primate Evolution: An Introduction to Man’s Place in Nature.” New York: MacMillan, 1972.

[2] T. Fukuda, H. Hosokai, and Y. Kondo, “Brachiation type of mobile robot,” in Fifth International Conference on Advanced Robotics’ Robots in Unstructured Environments. IEEE, 1991, pp. 915–920.

[3] K. Yamafuji, D. Fukushima, K. Maekawa. “Study of a mobile robot which can shift from one horizontal bar to another using vibratory excitation.” JSME Int. J., 35 (1992), pp. 456-461

[4] Spong, M.W., 1994. “Swing up control of the acrobat.” Proceedings IEEE International Conference on Robotics and Automation, pp. 2356–2361.

[5] T. Fukuda and F. Saito, “Motion control of a brachiation robot,”Robotics and autonomous systems, vol. 18, no. 1-2, pp. 83–93, 1996

[6] H. Kajima, Y. Hasegawa, T. Fukuda. “Learning algorithm for a brachiating robot.” Appl. Bionics Biomech., 1 (1) (2003), pp. 57-66

[7] A. Lo, Y.-H. Yang, T.-C. Lin, C.-W. Chu, and P.-C. Lin, “Model-based design and evaluation of a brachiating monkey robot with an active waist,” Applied Sciences, vol. 7, no. 9, p. 947, 2017.

[8] S. Farzan, A.-P. Hu, E. Davies, and J. Rogers, “Modeling and control of brachiating robots traversing flexible cables,” in 2018 IEEE International Conference on Robotics and Automation (ICRA). IEEE,2018, pp. 1645–1652

[9] S. Yang, Z. Gu, R. Ge, A.M. Johnson, M. Travers, H. Choset. “Design and Implementation of a Three-Link Brachiation Robot with Optimal Control Based Trajectory Tracking Controller” arXiv:1911.05168v1. Nov 2019.

[10] F. Michilsens, E.E. Vereecke, K. D’Aout, and P. Aerts, “Functional anatomy of the gibbon forelimb: adaptations to a brachiating lifestyle,” Journal of Anatomy, vol. 215, pp335-354, 2009.

[11] S.K.S. Thorpe, R.H. Crompton, M.M. Gunther, R.F. Ker, R. M. Alexander, “Dimensions and Moment Arms of the Hind- and Forelimb Muscles of Common Chimpanzees (*Pan troglodytes)*” American Journal of Physical Anthropology, 110: 179-199, 1999.

[12] J.B. Wells, “Comparison of mechanical properties between slow and fast mammalian muscles,” Journal of Physiology, 178, pp. 252-269, 1965.

[13] Y-H. Chang, J.E.A. Bertram, D.V. Lee, “External forces and torques generated by the brachiating white-handed gibbon (Hylobates lar),” American Journal of Physical Anthropology, 112:201-216, 2000.

Appendix

Table 1. Reference values for gibbon muscle

Muscle	Joint	Direction	PCSA [mm^2]	F_{max} [N]
Biceps major	Elbow	Flexion	523	157
Brachialis	Elbow	Flexion	618	185
Triceps	Elbow/ Shoulder	Extension/ Extension	253	75.9
Pectoralis major	Shoulder	Flexion	443	133
Deltoid	Shoulder	Both Flexion and Extension	1128	338
Latissimus dorsi	Shoulder	Extension	433	130